

Optimization for Hue Constant RGB Sensors

Graham D. Finlayson⁽¹⁾ and Sabine Süsstrunk^(1,2)

(1) School of Information Systems, University of East Anglia, Norwich, U.K.

(2) Laboratory for Audiovisual Communications, Swiss Federal Institute of Technology (EPFL), Lausanne, Switzerland

Abstract

We present an optimization technique to find hue constant RGB sensors. The hue representation is based on a log RGB opponent color space that is invariant to brightness and gamma. While modeling the visual response did not derive the opponent space, the hue definition is similar to the ones found in CIE Lab and IPT. Finding hue constant RGB sensors through this optimization might be applicable in color engineering applications such as finding RGB sensors for color image encodings.

Introduction

Hue is an important property of a color. As defined by the CIE, hue is the attribute of a visual sensation according to which an area appears to be similar to one of the perceived colors red, yellow, green and blue, or a combination of two of them [1]. In other words, it is the “name” of a color, and is one of the perceptual correlates like saturation and brightness.

Hue is the attribute of a color that people generally find easiest to identify. It is most often used to “describe” a color. Thus, segmenting images according to hue has been widely used for object segmentation, object recognition and image retrieval [2-4]. In the computer vision community, image RGB values are converted to a hue-based representation using a color transformation like HSV, HLS and IHS [5]. These transformations do not require a-priori knowledge about the RGB values, i.e. an exact definition linking RGB and tristimulus values (XYZ) is not needed. While not knowing the exact encoding parameters precludes the calculations of the CIE definition of hue, the results are acceptable for the applications mentioned above.

In the color imaging community, it has been noted that RGB color image encodings should have a high degree of hue constancy. In other words, a color ramp created by varying the encoding values to create different sensations in lightness or chroma (saturation) should still result in the same hue over the whole ramp. Additionally, simple non-linear channel editing should not affect the hue of a color [6]. In effect, hue constancy was one of the optimization criterion used in the development of the ROMM RGB color encoding [7]. The optimization was based on the CIE Lab hue definition.

In this paper, we are investigating if a hue based representation that is invariant to brightness and gamma [8], developed for the computer vision community, can be used to evaluate the hue constancy of RGB sensors. We use a spherical sampling method [9] to find a sensor set that maximizes straight hue lines for psycho-visually derived constant hue data [10] in a log RGB opponent color space. Using this definition of hue constancy, we also calculate the hue behavior of a number of sensors found in the color science and imaging community, such as ROMM [7], ITU-BT.R 709 [11], LMS, Sharp [12], Bradford [13], and color ratio stable sensors [14].

The hue definition of the log RGB opponent color space is similar to the hue definitions in other color spaces (see part 2). It has been successfully applied to image retrieval applications [8]. It is gamma invariant, i.e. the power function usually applied to any RGB encoding cancels out. However, XYZ based hue definitions, such as $H_{a^*b^*}$ [15] and H_{PT} of the IPT opponent encoding [16], are calculated with a power function. The power functions are equal to 1/3 and 0.43 for CIE Lab and IPT, respectively. Consequently, Lab $H_{a^*b^*}$ and IPT H_{PT} are strictly speaking only applicable to one given “contrast” encoding. While this contrast encoding is based on the encoding of the human visual system, it does not necessarily reflect other color image encodings that might be appropriate for certain applications like computer graphics.

We are not claiming here that the opponent log RGB hue definition is a more appropriate measure for defining visual hue constancy. However, it should be investigated as an appropriate tool to test hue constancy in terms of defining RGB color image encodings, i.e. it might be suitable for *color engineering* purposes as opposed to *color vision* modeling.

Brightness and Gamma Invariant Hue

The log RGB opponent color encoding [8] was developed on the following premise. In imaging applications, linear RGB signals captured by the digitizing device are usually encoded with a power function to compensate for system non-linearity such as the monitor transfer function. Therefore, the RGB vectors encoded for each pixel are equal to:

$$\begin{bmatrix} R \\ G \\ B \end{bmatrix} = \begin{bmatrix} \alpha R_{lin}^\gamma \\ \alpha G_{lin}^\gamma \\ \alpha B_{lin}^\gamma \end{bmatrix} \quad (1)$$

α is a scalar that compensates for the illuminance. Applying a log transform to the RGB values removes the γ term from the exponent and turns them into multiplicative scalars:

$$\log \begin{bmatrix} \alpha R_{lin}^\gamma \\ \alpha G_{lin}^\gamma \\ \alpha B_{lin}^\gamma \end{bmatrix} = \begin{bmatrix} \log(\alpha) + \gamma \log(R_{lin}) \\ \log(\alpha) + \gamma \log(G_{lin}) \\ \log(\alpha) + \gamma \log(B_{lin}) \end{bmatrix} \quad (2)$$

Brightness α becomes an additive rather than a multiplicative term. Taking differences of color channels, i.e. projecting orthogonal to the unitary vector (1,1,1) allows to remove the brightness term:

$$\begin{bmatrix} \log(\alpha) + \gamma \log(R_{lin}) \\ \log(\alpha) + \gamma \log(G_{lin}) \\ \log(\alpha) + \gamma \log(B_{lin}) \end{bmatrix} \mapsto \begin{bmatrix} \gamma \log(R_{lin}) - \gamma \log(G_{lin}) \\ \gamma \log(R_{lin}) + \gamma \log(G_{lin}) - 2\gamma \log(B_{lin}) \\ \gamma \log(R_{lin}) - \gamma \log(G_{lin}) \end{bmatrix} \quad (3)$$

Note that the definitions of the above differences describe coordinates in an opponent color representation. They are similar to the opponent color axes used by the human visual system and could be regarded as having perceptual relevance [17].

Finally, ratios of the opponent color coordinates are formed to cancel γ .

$$\frac{\gamma \log(R_{lin}) - \gamma \log(G_{lin})}{\gamma \log(R_{lin}) + \gamma \log(G_{lin}) - 2\gamma \log(B_{lin})} = \frac{\log(R_{lin}) - \log(G_{lin})}{\log(R_{lin}) + \log(G_{lin}) - 2\log(B_{lin})} \quad (4)$$

Hue is defined as the inverse tangent of the ratio of equation (4):

$$H = \tan^{-1} \frac{\log(R_{lin}) - \log(G_{lin})}{\log(R_{lin}) + \log(G_{lin}) - 2\log(B_{lin})} \quad (5)$$

The definition of hue is very similar to the CIE $H_{a^*b^*}$ definition, which defines hue as the inverse tangent of the ratio of the opponent color coordinates b^* (blue-yellow) and a^* (red-green). What is noteworthy about equation (5) is that it follows only from the engineering imperative to cancel brightness and gamma. There was no attempt made to model visual response. Rather, mathematically deriving gamma and brightness independence led to a visual system like definition of hue.

Experiment

The goal of this experiment was to find RGB sensors that keep hue constant and to evaluate the hue constancy of known sensors. As initial data sets, we used the hue-constant data published by Hung and Berns [10]. They derived XYZ tristimulus values, four values at each hue angle for 12 hue

angles, through a psychovisual experiment on a CRT monitor. The resulting data set has been extensively used to test hue constancy in color appearance models and color encodings. The original data set was defined under illuminant C. We used a Sharp chromatic adaptation transform [12] to calculate the corresponding colors under illuminant D65, so that the results better correspond to previous hue-constancy experiments [6,16].

A spherical sampling technique as described in [9] was applied to find the best sensor that keeps hue most constant. In the case of trichromatic (RGB and XYZ) imaging applications, the basis functions span a three-dimensional space. If the lengths of the vectors are normalized to unity, then different vector combinations can be illustrated with their end-points that lie on the surface of a sphere. Trying all possible combinations of three points distributed over the surface of the sphere allows finding all possible solutions to a given problem. In this experiment, three different points on the sphere represent three different RGB sensors. The linear transformation T from XYZ to RGB can be calculated according to the method described in [9].

Out of computational consideration, we only tested sensors that had their endpoints located within 30 degrees of the ITU BT.R. 709 and ROMM red, green, and blue sensors, resulting in ~6 million different RGB sensor sets (**I**) to be tested (see Figure 1). The ITU BT.R. 709 sensors are the basis for sRGB [18], and the ROMM sensors the basis for ROMM RGB [19], two color encodings that are widely used and are considered to be somewhat hue constant.

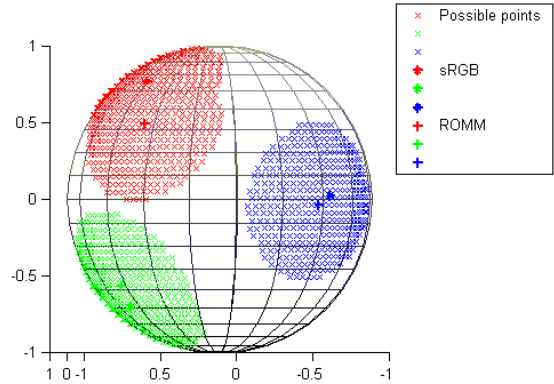


Figure 1: Sample points around 30 degrees of the ITU-R.BT 709 and ROMM sensors considered in the optimization

The hue-constant XYZ values were converted to linear RGB using the (3x3) linear transforms T found through the spherical sampling technique. The Hung & Berns data set consists of 12 hue angles, with four points for each hue, resulting in 48 XYZ values.

If P is a (48x3) matrix of normalized XYZ values, and S is a (48x3) matrix of linear RGB values, then:

$$S = PT \quad (6)$$

Not all transforms result in positive R, G, and B values. Before converting to log space, the values need to be offset to render them all positive. This offset can be considered as adding brightness to the RGB channels, or defining a different encoding range. In effect adding an offset amounts to a “gamut mapping algorithm.” Indeed, amongst the entire gamut mapping approaches we might have considered, this is the simplest. Other approaches might be applied, including a compression curve where only values close to 0 are brightened. This latter approach has the advantage of retaining the meaning of the log operator (and so keeping to the engineering definition of hue).

Once all the RGB values are rendered positive, the log RGB opponent color matrix \mathbf{O} (48x2) can then be calculated as described in equations (2) and (3).

Perfectly hue constant data in an opponent color encoding should have the same hue angle. Data points with equal hue should thus lie on a line going through the origin (see Figure 2). Calculating the deviation from the line, i.e. how far the data points actually are from the line representing the hue angle, gives an indication of hue constancy. Therefore, the problem of finding the most hue constant RGB sensor can be expressed as a line-fitting problem.

Using singular value decomposition, we can find a line that best fits a set of data points minimizing least squares error. However, we have the additional constraint that the line needs to go through the origin. Adding a “mirrored” point to each of the opponent log RGB matrix entries will result in a hue matrix \mathbf{H} (96x2) with a mean equal to zero:

$$\mathbf{H} = [\mathbf{O}; \mathbf{O} \times (-1)] \quad (7)$$

For better comparisons between the different sensor results, \mathbf{H} was transformed linearly to a new matrix $\tilde{\mathbf{H}}$ that is “white,” i.e. its components are uncorrelated and their variances equal unity. From equation (7) it is clear that \mathbf{H} is already centered, i.e. it has zero mean. Therefore, the “whitening” transformation is based on the eigenvalue decomposition of the covariance matrix ($\mathbf{H}^T \mathbf{H}$) of \mathbf{H} :

$$\mathbf{H}^T \mathbf{H} = \mathbf{E} \Lambda \mathbf{E}^T \quad (8)$$

where \mathbf{E} is a matrix of eigenvectors, and Λ is a diagonal matrix of eigenvalues. $\tilde{\mathbf{H}}$ is calculated as follows:

$$\tilde{\mathbf{H}} = \mathbf{H} (\mathbf{E} \Lambda^{-1/2})^T \quad (9)$$

As the best fitting line has to be calculated for each hue angle separately, $\tilde{\mathbf{H}}$ was divided into n ($n=12$) matrices $\tilde{\mathbf{H}}_n$ (8x2), each containing four hue points and four mirrored points that should lie on the same hue line. The singular value decomposition of $\tilde{\mathbf{H}}_n$ can then be written as:

$$\tilde{\mathbf{H}}_n = \mathbf{U}_n \mathbf{D}_n \mathbf{V}_n^T \quad (10)$$

where \mathbf{U}_n and \mathbf{V}_n are singular vector matrices and \mathbf{D}_n is a diagonal matrix of singular values:

$$\mathbf{D}_n = \begin{bmatrix} \sigma_1 \\ \sigma_2 \end{bmatrix}$$

The second singular value, σ_2 , is the residual error, i.e. the distance of the actual points to the line that best fits the data.

The mean residual error ε of one sensor set was calculated by averaging over the individual residual errors of the 12 hue lines, such that:

$$\varepsilon = \frac{1}{n} \sum_{n=1}^{12} \sigma_2(n) \quad (11)$$

Minimizing the mean residual error ε derived the best sensor of the original sensor sets \mathbf{I} found through the spherical sampling technique:

$$\mathbf{s}_{\text{opt}} = \arg \min_{\mathbf{s}_{\text{opt}} \in \mathbf{I}} (\varepsilon) \quad (12)$$

The result of the spherical optimization is illustrated in Figure 2, and the corresponding sensors \mathbf{s}_{opt} in Figure 3.

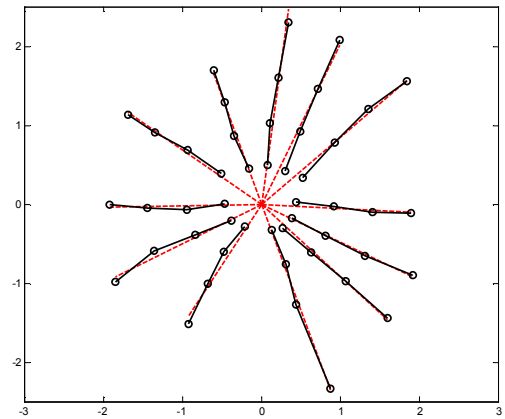


Figure 2: Best hue constancy found through the spherical sampling technique. The mean residual error is equal to 0.0884.

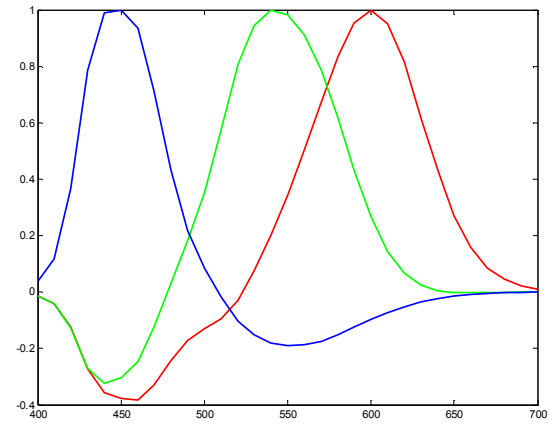


Figure 3: Sensors that result in the best hue constancy found through the spherical sampling technique.

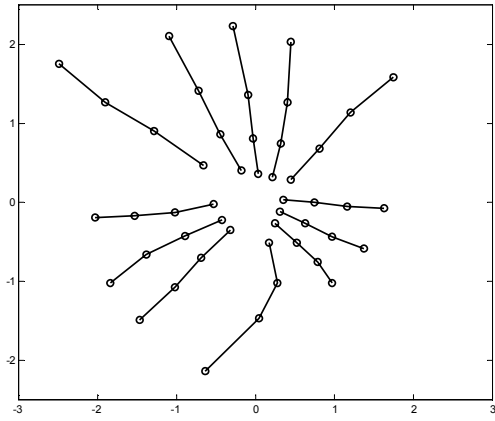


Figure 4: Hue constancy for the ROMM sensors. The mean residual error is equal to 0.1686.

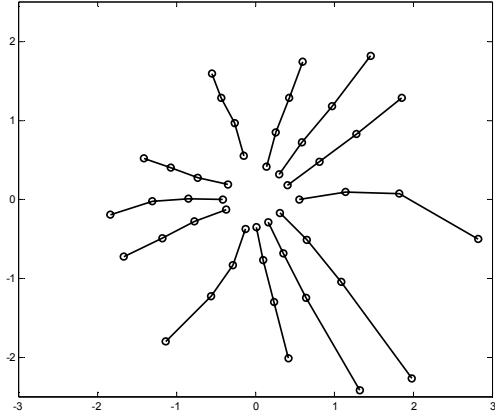


Figure 5: Hue constancy for the 709 sensors. The mean residual error is equal to 0.1653.

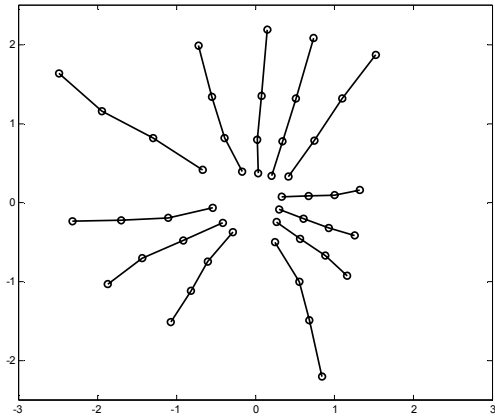


Figure 6: Hue constancy for the LMS sensors. The mean residual error is equal to 0.1039.

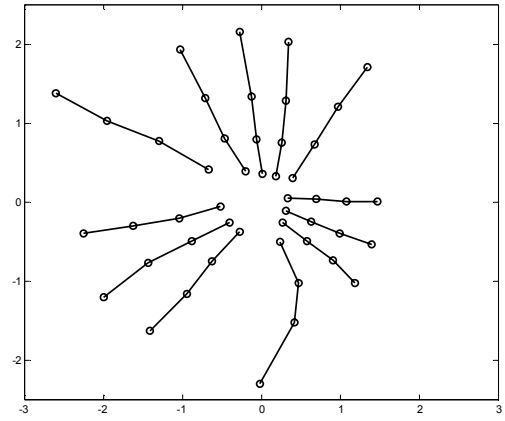


Figure 7: Hue constancy for the Sharp sensors [12]. The mean residual error is equal to 0.1504.

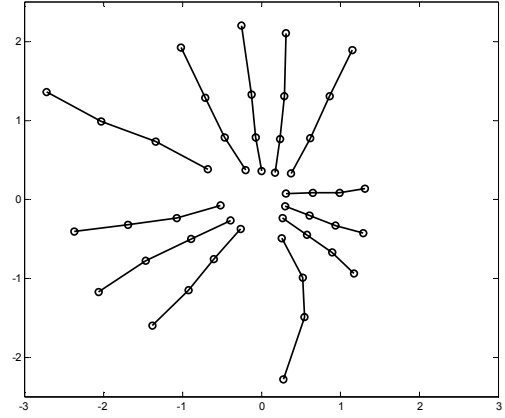


Figure 8: Hue constancy for the Bradford sensors [13]. The mean residual error is equal to 0.1423.

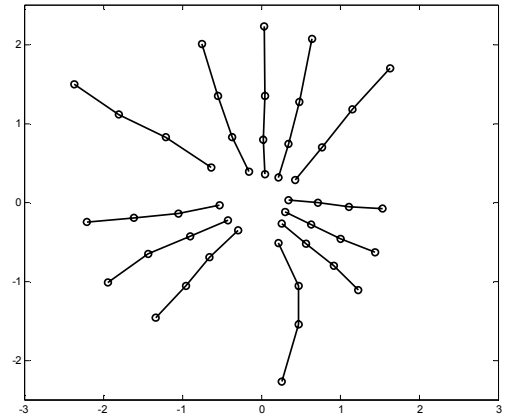


Figure 9: Hue constancy for the sharp sensors that keep color ratios most stable over different illuminants [14]. The mean residual error is equal to 0.1244.

The corresponding sensors found through this experiment have relatively large negative values and are probably not specifically suited to imaging applications. As a comparison, the hue constancy of the ROMM RGB, ITU-BT.R 709, LMS, derived by the Hunt-Pointer-Estevez transformation, the Sharp and Bradford sensors used in chromatic adaptation transforms [12,13], and the sharp sensors that keep color ratios most stable over different illuminants [14] are also plotted (see Figures 4-9). These latter sensors are all white-point preserving, i.e. equal X, Y, and Z values are mapped to equal R, G, and B values.

Conclusions

We have presented an optimization technique that can evaluate the hue constancy of RGB sensors. We base our experiment on the psycho-visually derived hue constant data from Hung and Berns. Hue constancy is evaluated in a log RGB opponent color encoding that has been developed for the computer vision community. The most hue constant RGB sensors were found through a spherical sampling technique.

The experimental procedure presented in this paper has many degrees of freedom. The offset term used to avoid negative RGB values has an influence on the final result, as well as the whitening. The error term to be minimized could be refined to take the lengths of the hue vectors or the correlation of the RGB sensors into account. However, the method is very flexible, and can be used for hue definition independent of gamma and white-point encoding. Note that both Lab $H_{a^*b^*}$ and IPT H_{PT} are contrast dependent, and IPT additionally requires a white-point of D65. Indeed, our paper could be regarded as a continuation of the work of Ebner and Fairchild on IPT to find a generalized model for evaluating hue constancy for color engineering purposes.

Additionally, other hue constant test data should also be evaluated. The Hung and Berns data has a limited number of tristimulus values. The “blue” hue vector pointing to the x-axis in Figures 4-9 is not very straight for almost all the sensors, which adds a significant amount to the residual error. It is not clear from this study if this is due to the sensors or noise in the test data.

While there is more investigation needed if this log RGB representation can be used to define hue constancy for color imaging applications, we can already make the following observations. A log RGB opponent encoding would allow evaluating hue constancy independent of any contrast (gamma) corrections. Sharp sensors seem to be almost as hue constant as correlated sensors, such as LMS, in this representation. This emphasizes again the results of previous investigations, where sharp sensors were found to be optimal in predicting corresponding color data, and in keeping color ratios over different illuminants constant. There seem to be many indicators that sharp sensors do play a role in color engineering.

References

- [1] CIE, *International Lighting Vocabulary*, CIE Publication 17.4, Commission Internationale de l'Eclairage, 4th edition, 1989.
- [2] F. Perez and C. Koch, “Hue color segmentation determines object boundaries,” *Int. J. Computer Vision*, 12, 1994.
- [3] T. Gevers and A.W.M. Smeulders, “Color based object recognition,” *Pattern Recognition*, 32, pp. 453-464, 1999.
- [4] B.M. Mehtre, M.S. Kankanhalli, A.D. Narasimhalu, and G.C. Man, “Color matching for image retrieval,” *Pattern Recognition Letters*, 16(3), pp. 325-331, 1995.
- [5] J. Sangwine and R.E.N. Horne, *The Colour Image Processing Handbook*, Chapman & Hall, 1998.
- [6] N. Morony, “Hue constancy of RGB spaces,” *Proc. IS&T/SID 9th Color Imaging Conference*, pp. 163-167, 2001.
- [7] K.E. Spaulding, G.J. Woolfe, and E.J. Giorgianni, “Optimized extended gamut color encoding for scene-referred and output-referred image states,” *J. Imaging Science and Technology*, 45(5), pp. 418-426, 2001.
- [8] G. Finlayson and G. Schaefer, “Hue that is invariant to brightness and gamma,” *Proc. British Machine Vision Conference*, pp. 303-312, 2000.
- [9] G.D. Finlayson and S. Süsstrunk, “Spherical sampling and color transformations,” *Proc. IS&T/SID 9th Color Imaging Conference*, pp. 321-325, 2001.
- [10] P. Hung and R. Berns, “Determination of constant hue loci for a CRT gamut and their prediction using color appearance spaces,” *Color Research and Applications*, 20, pp. 285-295, 1995.
- [11] ITU-R Recommendation BT.709-3: 1998, *Parameter values for the HDTV standards for production and international programme exchange*.
- [12] G.D. Finlayson and S. Süsstrunk, “Performance of a chromatic adaptation transform based on spectral sharpening,” *Proc. IS&T/SID 8th Color Imaging Conference*, pp.49-55, 2000.
- [13] K.M. Lam, “Metamerism and Colour Constancy,” Ph.D. Thesis, University of Bradford, 1985.
- [14] G.D. Finlayson and S. Süsstrunk, “Color ratios and chromatic adaptation.” *Proc. IS&T CGIV*, pp.7-10, 2002.
- [15] CIE, *Colorimetry*, CIE Publication 15.2, Commission Internationale de l'Eclairage, 2nd edition, 1986.
- [16] F. Ebner and M. Fairchild, “Development and testing of a color space (IPT) with improved hue uniformity,” *Proc. IS&T/SID 6th Color Imaging Conference*, pp. 8-13, 1998.
- [17] L. Hurvich and D. Jameson, “An opponent-process theory of color vision,” *Psychological Review*, 64, pp.384-390, 1957.
- [18] IEC 61966-2-1 (1999): *Multimedia systems and equipment – Colour measurement and management – Part 2-1: Colour management – Default RGB colour space – sRGB*.
- [19] PIMA 7666: 2001 Photography – *Electronic Still Picture Imaging – Reference Output Medium Metric RGB Color encoding: ROMM-RGB*.